Available online at www.sciencedirect.com

ScienceDirect

Mendeleev Commun., 2023, **33**, 86–89

Mendeleev Communications

Effect of stereocomplex formation between enantiomeric poly(L,L-lactide) and poly(D,D-lactide) blocks on self-organization of amphiphilic poly(lactide)-*block*-poly(ethylene oxide) copolymers in dilute aqueous solution

Anastasiia M. Desyatskova,[a] Ekaterina V. Kuznetsova,*[a] Yulia A. Puchkova,[a,b] Evgeny V. Yastremsky,[a,c] Artem V. Bakirov,[a,b] Petr V. Dmitryakov,[a] Alexander I. Buzin[b] and Sergei N. Chvalun[a,b]

[a] *National Research Center 'Kurchatov Institute', 123182 Moscow, Russian Federation. E-mail: kuznetsova.kate992@gmail.com*

[b] *N. S. Enikolopov Institute of Synthetic Polymeric Materials, Russian Academy of Sciences, 117393 Moscow, Russian Federation*

[c] *A. V. Shubnikov Institute of Crystallography, Federal Research Center 'Crystallography and Photonics', Russian Academy of Sciences, 119333 Moscow, Russian Federation*

DOI: 10.1016/j.mencom.2023.01.027

The effect of crystallization of a hydrophobic poly(lactide) block on the self-organization of biocompatible and biodegradable amphiphilic poly(lactide)-*block*-poly(ethylene oxide) (PLA-*b*-PEO) copolymers in a dilute aqueous solution has been investigated. It was demonstrated that the co-crystallization of poly(L,L-lactide) [P(L,L)LA] and poly(D,D-lactide) [P(D,D)LA] chains under equimolar mixing of P(L,L)LA$_{46}$-*b*-PEO$_{113}$ and P(D,D)LA$_{56}$-*b*-PEO$_{113}$ copolymers resulted in the formation of stable and spontaneously water-redispersible stereocomplex micelles with semicrystalline P(L,L)LA/P(D,D)LA cores. It was shown that the P(L,L)LA$_{46}$/P(D,D)LA$_{56}$-*b*-PEO$_{113}$ stereocomplex micelles produced by dialysis can be potential vehicles for the anticancer agent oxaliplatin.

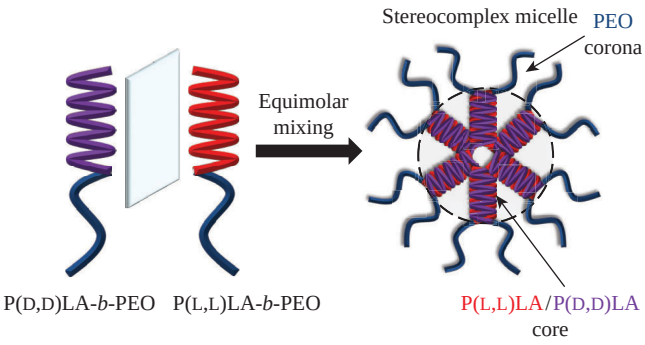

Keywords: amphiphilic block copolymers, poly(lactide), poly(ethylene oxide), self-organization, stereocomplex formation, block copolymer micelles, drug delivery systems.

In recent decades, the self-organization of biocompatible and biodegradable amphiphilic block copolymers of lactide (LA) and ethylene oxide (EO) in aqueous solution into nanosized micelles with the 'core–corona' structure has been extensively investigated.[1–4] Micelles based on poly(lactide)/poly(ethylene oxide) (PLA/PEO) block copolymers of various molecular composition are promising vehicles for targeted delivery of different drugs, including anticancer ones.[5–7] It was previously shown that the encapsulation efficiency (EE) of the lipophilic anticancer agent oxaliplatin in micelles of an amphiphilic block copolymer of D,L-lactide (D,L-LA) and EO [P(D,L)LA$_{62}$-*b*-PEO$_{113}$] was about 76%,[5] while the EE of oxaliplatin in nanoparticles of a hydrophobic copolymer of D,L-LA and glycolide with the D,L-LA/glycolide molar ratio of 90 : 10 did not exceed 8.7%.[8] Encapsulation of drug molecules in PLA-*b*-PEO micelles makes it possible to increase the water solubility, stability and bioavailability of drugs, as well as to prolong their circulation time in the body due to the 'stealth effect' of the PEO corona, which minimizes the recognition and elimination of carriers by the reticuloendothelial system.

The structure and physicochemical properties such as size, shape, stability, encapsulation capacity, release rate of encapsulated molecules and degradation rate of PLA-based materials can be varied over a wide range by changing the polymer architecture,[2] its molecular weight,[9] the length ratio of hydrophilic and hydrophobic blocks[5,10] and also the stereoregularity of the hydrophobic PLA block.[2,11] Three types of PLA, *i.e.* non-stereospecific amorphous poly(D,L-lactide) [P(D,L)LA] and stereospecific crystallizing poly(L,L-lactide) [P(L,L)LA] and poly(D,D-lactide) [P(D,D)LA] can be synthesized from different stereoisomers of LA. Crystallization of the PLA block significantly affects the self-organization of PLA-*b*-PEO copolymers in aqueous solution. Jelonek *et al.* showed that P(L,L)LA$_x$-*b*-PEO$_{114}$ (x = 54–85) copolymers with crystallizable P(L,L)LA blocks are capable of forming extended micelles in aqueous solution, while the P(D,L)LA$_{80}$-*b*-PEO$_{114}$ copolymer with amorphous P(D,L)LA block gave only spherical ones.[12] P(L,L)LA$_{64}$-*b*-PEO$_{113}$ micelles with semicrystalline P(L,L)LA cores were reported[13] to exhibit twice the EE of the model drug doxorubicin than P(D,L)LA$_{58}$-*b*-PEO$_{113}$ micelles with amorphous P(D,L)LA cores (16.6 ± 1.3 and 8.1 ± 1.1 %, respectively). On the contrary, the release of loaded doxorubicin *in vitro* was faster for amorphous P(D,L)LA$_{58}$-*b*-PEO$_{113}$ micelles. Moreover, equimolar mixing of the crystallizable P(L,L)LA-*b*-PEO and P(D,D)LA-*b*-PEO copolymers in an aqueous solution led to the formation of micelles with cores consisting of the P(L,L)LA/P(D,D)LA stereocomplex as a result of

Table 1 Physicochemical characteristics of the PLA_n-*b*-PEO_{113} micelles.

Sample	CMC/M	D_h^a/nm	$2R^b$/nm	D^c/nm	ζ^d/mV
P(L,L)LA_{46}-*b*-PEO_{113}	$(2.4 \pm 0.8) \times 10^{-7}$	32 ± 7	9 ± 2	17 ± 5	–13.4 ± 0.8
P(L,L)LA_{46}/P(D,D)LA_{56}-*b*-PEO_{113}	$(2.0 \pm 0.5) \times 10^{-7}$	30 ± 7	11 ± 2	13 ± 2	–5.0 ± 0.3
P(D,L)LA_{66}-*b*-PEO_{113}	$(2.5 \pm 0.6) \times 10^{-7}$	44 ± 9	n.a.	21 ± 5	–27.4 ± 0.9

[a] Hydrodynamic diameter of block copolymer micelles, defined as the value corresponding to the first peak on the DLS intensity (*I*, %) size distribution curve. [b] Scattering object size calculated from SAXS data. [c] Diameter of block copolymer micelles evaluated from TEM images. [d] Electrokinetic potential of block copolymer micelles.

co-crystallization of P(L,L)LA and P(D,D)LA chains.[14–16] Stereocomplex micelles usually exhibit higher thermodynamic and kinetic stability, as well as they are less prone to aggregation during lyophilization, which makes them promising vehicles for drug delivery.[17,18]

In this work, we obtained micelles from the semicrystalline P(L,L)LA_{46}-*b*-PEO_{113} copolymer, an equimolar mixture of semicrystalline P(L,L)LA_{46}-*b*-PEO_{113} and P(D,D)LA_{56}-*b*-PEO_{113} copolymers, as well as the amorphous P(D,L)LA_{66}-*b*-PEO_{113} copolymer to elucidate the effect of crystallization and stereocomplexation of the hydrophobic PLA block on the structure of the micellar core, the size, morphology and stability of micelles, as well as their ability to encapsulate the anticancer agent oxaliplatin.

The block copolymers were synthesized† by ring-opening polymerization of L,L-, D,D- or D,L-lactide in the presence of PEO methyl ether with a number average molecular weight (M_n) of 5 kDa according to a standard procedure.[19] Stannous 2-ethylhexanoate was used as a catalyst. Molecular characteristics of the synthesized polymers (Table S1†) were determined using ^{1}H nuclear magnetic resonance and gel permeation chromatography.† The thermal stability and thermophysical properties of the copolymers were studied using thermogravimetric analysis (Figure S1†) and differential scanning calorimetry (DSC) (Figure S2). According to DSC data, the degree of crystallinity of the hydrophobic P(L,L)LA and P(D,D)LA blocks in the P(L,L)LA_{46}-*b*-PEO_{113} and P(D,D)LA_{56}-*b*-PEO_{113} copolymers is 27 and 35%, respectively (Table S2).

Aqueous dispersions of block copolymer micelles were prepared by dialyzing a solution of the block copolymer or an equimolar mixture of copolymers in tetrahydrofuran (a non-selective organic solvent) against bidistilled water at room temperature for one week using a dialysis tube with MWCO = 3.5 kDa.†

Critical micelle concentration (CMC) of P(L,L)LA_{46}-*b*-PEO_{113}, P(D,L)LA_{66}-*b*-PEO_{113}, as well as an equimolar mixture of P(L,L)LA_{46}-*b*-PEO_{113} and P(D,D)LA_{56}-*b*-PEO_{113} copolymers was determined by fluorescence spectroscopy according to the standard procedure.†,[20] All samples have low CMC values of approximately

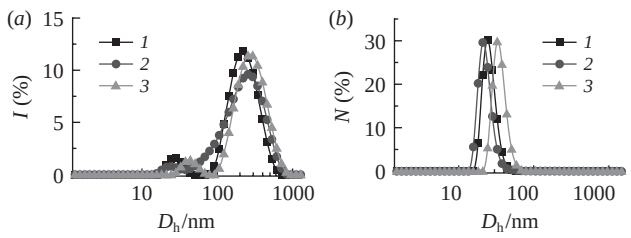

Figure 1 Size distribution curves of (*a*) DLS intensity and (*b*) DLS numbers for aqueous dispersions of (*1*) P(L,L)LA_{46}-*b*-PEO_{113} copolymer, (*2*) an equimolar mixture of P(L,L)LA_{46}-*b*-PEO_{113} and P(D,D)LA_{56}-*b*-PEO_{113} copolymers and (*3*) P(D,L)LA_{66}-*b*-PEO_{113} copolymer (c = 1 g dm^{-3}).

† For details, see Online Supplementary Materials.

$(2.0–2.5) \times 10^{-7}$ M (Table 1). Thus, it can be assumed that the block copolymer micelles are thermodynamically stable.

Aqueous micellar dispersions were studied by dynamic light scattering (DLS).† The DLS intensity size distribution curves for all PLA_n-*b*-PEO_{113} micelles reveal two peaks [Figure 1(*a*)], which can be attributed to small individual micelles (D_h < 100 nm) and their aggregates (D_h > 100 nm). Since the intensity of light scattering of large objects is sufficiently higher than that of small objects,[21] and peaks corresponding to individual micelles are detected [see Figure 1(*a*)], we suppose that the main fraction of individual 'core–corona' PLA_n-*b*-PEO_{113} micelles co-exists with a minor fraction of aggregates. This assumption is qualitatively confirmed by the DLS number size distribution curves [Figure 1(*b*)].

The D_h values of individual P(L,L)LA_{46}-*b*-PEO_{113}, P(L,L)LA_{46}/P(D,D)LA_{56}-*b*-PEO_{113} and P(D,L)LA_{66}-*b*-PEO_{113} micelles are presented in Table 1. It can be seen that the micelles based on the amorphous P(D,L)LA_{66}-*b*-PEO_{113} copolymer have a higher D_h value compared to the micelles of the semicrystalline P(L,L)LA_{46}-*b*-PEO_{113} copolymer and those based on the equimolar mixture of P(L,L)LA_{46}-*b*-PEO_{113} and P(D,D)LA_{56}-*b*-PEO_{113}, which could be attributed to the different stereoregularity of the hydrophobic PLA block and, consequently, to the different structure of the micellar core. It is known that the crystallization of hydrophobic PLA chains in the micellar core can favour their dense packing, which leads to a decrease in the size of micelles.[14]

The electrokinetic potential (ζ potential) of PLA_n-*b*-PEO_{113} micelles is negative (see Table 1), which can be explained by the dissociation of PLA carboxyl groups on the surface of the micellar core.[22]

The crystalline structure of the P(L,L)LA_{46}-*b*-PEO_{113} and P(L,L)LA_{46}/P(D,D)LA_{56}-*b*-PEO_{113} micelles was studied by wide-angle X-ray scattering (WAXS) (Figure 2).† The diffraction patterns show Bragg peaks corresponding to the (111/120) and (112) reflections of the crystalline PEO block[19] (see Figure 2). For the P(L,L)LA_{46}-*b*-PEO_{113} micelles, the (200/110) reflection of the α-form of P(L,L)LA[19] was also found, while for the P(L,L)LA_{46}/P(D,D)LA_{56}-*b*-PEO_{113} micelles, (110) and (300/030) reflections of the P(L,L)LA/P(D,D)LA stereocomplex[17] are observed. As can be seen from Figure 2, the intensity of the (110) reflection of the P(L,L)LA/P(D,D)LA stereocomplex is higher than that of the (200/110) reflection of P(L,L)LA, which qualitatively refers to a higher degree of crystallinity of the P(L,L)LA_{46}/P(D,D)LA_{56}-*b*-PEO_{113} micellar core.

Aqueous dispersions of the semicrystalline P(L,L)LA_{46}-*b*-PEO_{113} copolymer and the equimolar mixture of P(L,L)LA_{46}-*b*-PEO_{113} and P(D,D)LA_{56}-*b*-PEO_{113} copolymers were studied by small-angle X-ray scattering (SAXS).† Experimental scattering curves for the P(L,L)LA_{46}-*b*-PEO_{113} and P(L,L)LA_{46}/P(D,D)LA_{56}-*b*-PEO_{113}

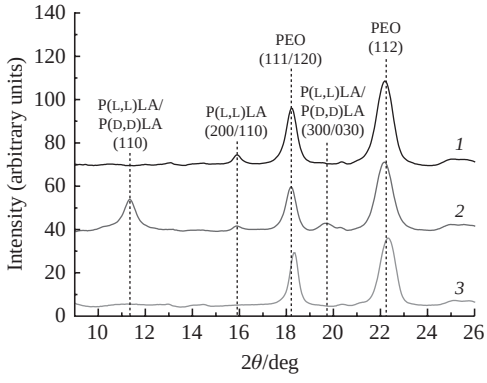

Figure 2 WAXS patterns of freeze-dried micelles based on (*1*) P(L,L)LA_{46}-*b*-PEO_{113} copolymer, (*2*) an equimolar mixture of P(L,L)LA_{46}-*b*-PEO_{113} and P(D,D)LA_{56}-*b*-PEO_{113} copolymers and (*3*) P(D,L)LA_{66}-*b*-PEO_{113} copolymer. The curves are shifted vertically for clarity.

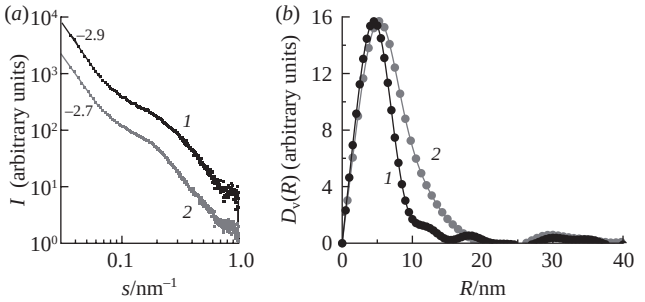

Figure 3 (*a*) Experimental SAXS curves plotted in the coordinates log *I vs.* log *s* for micelles based on (*1*) P(L,L)LA$_{46}$-*b*-PEO$_{113}$ copolymer and (*2*) an equimolar mixture of P(L,L)LA$_{46}$-*b*-PEO$_{113}$ and P(D,D)LA$_{56}$-*b*-PEO$_{113}$ copolymers, together with (*b*) the corresponding volume size distribution functions $D_v(R)$.

micelles plotted in the coordinates log *I vs.* log *s* are presented in Figure 3(*a*). The SAXS curves show straight segments in the region of the momentum transfer $s < 0.06$ nm^{-1} for the P(L,L)LA$_{46}$-*b*-PEO$_{113}$ and P(L,L)LA$_{46}$/P(D,D)LA$_{56}$-*b*-PEO$_{113}$ micelles with the slope value (*k*) of -2.9 ± 0.1 and -2.7 ± 0.1, respectively, which may indicate the presence of large scattering objects (aggregates) in the dispersions.[23]

The volume size distribution functions $D_v(R)$ of the scattering objects were calculated from the experimental SAXS curves [Figure 3(*b*)]. As can be seen, objects with a radius $R \sim 5$ nm make up the main fraction in the aqueous dispersions. The size ($2R$) of scattering objects calculated from the SAXS data is lower than the D_h values of the P(L,L)LA$_{46}$-*b*-PEO$_{113}$ and P(L,L)LA$_{46}$/P(D,D)LA$_{56}$-*b*-PEO$_{113}$ micelles evaluated using DLS (see Table 1). It should be noted that the main contribution to X-ray scattering is made by the PLA core, while the contribution of the PEO corona is less pronounced due to its lower electron density.

The morphology of PLA$_n$-*b*-PEO$_{113}$ micelles was studied by transmission electron microscopy (TEM) (Figure 4).† After casting an aqueous dispersion of the semicrystalline P(L,L)LA$_{46}$-*b*-PEO$_{113}$ copolymer onto a solid substrate, the co-existence of individual spherical micelles with a diameter (D) of 17 ± 5 nm and band-like structures with a thickness of 15 ± 3 nm and a length from 100 nm to several microns was revealed [Figure 4(*a*)]. In the case of the equimolar mixture of P(L,L)LA$_{46}$-*b*-PEO$_{113}$ and P(D,D)LA$_{56}$-*b*-PEO$_{113}$ copolymers, the main fraction, consisting of individual spherical particles with $D = 13 \pm 2$ nm [Figure 4(*b*)], and the minor fraction, consisting of large, branched, irregularly shaped aggregates [Figure 4(*c*)], were identified. The formation of such structures has been previously reported.[24] For the amorphous P(D,L)LA$_{66}$-*b*-PEO$_{113}$ copolymer, only spherical micelles were found (Figure S3). TEM image analysis (Figure S4) showed that the D value of micelles of the P(L,L)LA$_{46}$/P(D,D)LA$_{56}$-*b*-PEO$_{113}$ stereocomplex is smaller than that of P(L,L)LA$_{46}$-*b*-PEO$_{113}$ and P(D,L)LA$_{66}$-*b*-PEO$_{113}$ micelles (see Table 1), which can be explained by stereocomplexation leading to dense packing of P(L,L)LA and P(D,D)LA chains both due to Van der Waals forces,[25] and due to the formation of intermolecular hydrogen bonds[26] in the micellar core.

It is known that block copolymer micelles with a semicrystalline core can recrystallize and form new crystalline structures upon

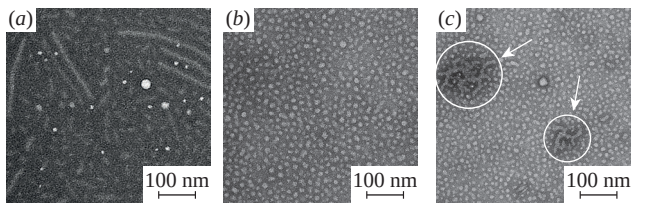

Figure 4 Typical TEM images of micelles based on (*a*) P(L,L)LA$_{46}$-*b*-PEO$_{113}$ copolymer and (*b*),(*c*) an equimolar mixture of P(L,L)LA$_{46}$-*b*-PEO$_{113}$ and P(D,D)LA$_{56}$-*b*-PEO$_{113}$ copolymers ($c = 0.5$ g dm^{-3}).

immobilization of a dispersion on a substrate. The morphology of these structures depends on the tethering density of the hydrophilic corona chains and the corona thickness.[2] To clarify this, we estimated the area of the crystalline PLA core per one tethered PEO chain (s) and the tethering density of the PEO corona (σ) for the micelles of P(L,L)LA$_{46}$-*b*-PEO$_{113}$ and P(L,L)LA$_{46}$/P(D,D)LA$_{56}$-*b*-PEO$_{113}$ (Table S3). It was found that the P(L,L)LA$_{46}$-*b*-PEO$_{113}$ micelles are characterized by a lower s value and, consequently, a higher σ value compared to the P(L,L)LA$_{46}$/P(D,D)LA$_{56}$-*b*-PEO$_{113}$ stereocomplex micelles (see Table S3). We suppose that the higher tethering density of the PEO corona on the crystalline P(L,L)A core results in a higher degree of stretching of the PEO chains in the P(L,L)LA$_{46}$-*b*-PEO$_{113}$ micellar corona, which favours the formation of band-like structures on the substrate [see Figure 4(a)] with larger s per one PEO chain.

The nanosomal form of the anticancer agent oxaliplatin was produced based on the P(L,L)LA$_{46}$-*b*-PEO$_{113}$/P(D,D)LA$_{56}$-*b*-PEO$_{113}$ stereocomplex micelles† due to their stability over a wide range of dispersion concentrations (Figure S5). Moreover, the D_h values of the P(L,L)LA$_{46}$/P(D,D)LA$_{56}$-*b*-PEO$_{113}$ micelles remained unchanged (within the experimental uncertainty) for two weeks (Figure S6), which indicates the kinetic stability of the micelles. The drug loading content (DLC) in the P(L,L)LA$_{46}$/P(D,D)LA$_{56}$-*b*-PEO$_{113}$ micelles was determined using inductively coupled plasma mass spectrometry.† The DLC value was 1.26 wt% (the initial DLC was 5 wt% with respect to the total weight of the copolymers), the efficiency of encapsulation of oxaliplatin in the micelles reached 25.2%. Loading with oxaliplatin did not affect the D_h values of the micelles (data not shown). Freeze-dried P(L,L)LA$_{46}$/P(D,D)LA$_{56}$-*b*-PEO$_{113}$ micelles loaded with oxaliplatin are capable of spontaneous redispersion without the use of any cryoprotectants (Figure S7), whereas freeze-dried P(L,L)LA$_{46}$-*b*-PEO$_{113}$ and P(D,L)LA$_{66}$-*b*-PEO$_{113}$ micelles are not able to redisperse to their original size in the absence of any cryoprotectants (see Figure S7). Thus, it can be assumed that micelles of the PLA-*b*-PEO stereocomplex are promising candidates for targeted drug delivery.

In this work, WAXS, SAXS, DLS and TEM methods were used to investigate the effect of crystallization of P(L,L)LA chains and co-crystallization of P(L,L)LA and P(D,D)LA chains on the structure of the semicrystalline core of P(L,L)LA$_{46}$-*b*-PEO$_{113}$ and P(L,L)LA$_{46}$/P(D,D)LA$_{56}$-*b*-PEO$_{113}$ micelles, respectively, as well as their size and morphology. It was found that P(L,L)LA$_{46}$-*b*-PEO$_{113}$ and P(L,L)LA$_{46}$/P(D,D)LA$_{56}$-*b*-PEO$_{113}$ micelles with semicrystalline P(L,L)LA and P(L,L)LA/P(D,D)LA cores, respectively, have smaller hydrodynamic diameters than P(D,L)LA$_{66}$-*b*-PEO$_{113}$ micelles with amorphous P(D,L)LA cores, which can be attributed to the looser packing of P(D,L)LA chains in the latter case. Using TEM, it was shown that individual P(L,L)LA$_{46}$-*b*-PEO$_{113}$ micelles tend to recrystallize with the formation of new crystalline band-like structures upon casting the dispersion onto a substrate, while upon the immobilization of a dispersion of P(L,L)LA$_{46}$/P(D,D)LA$_{56}$-*b*-PEO$_{113}$ stereocomplex micelles on a substrate, individual spherical micelles co-exist with a minor amount of irregularly shaped clusters. Freeze-dried P(L,L)LA$_{46}$/P(D,D)LA$_{56}$-*b*-PEO$_{113}$ micelles were shown to be capable of spontaneous redispersion without the use of any cryoprotectants, in contrast to P(L,L)LA$_{46}$-*b*-PEO$_{113}$ and P(D,L)LA$_{66}$-*b*-PEO$_{113}$ micelles. Moreover, P(L,L)LA$_{46}$/P(D,D)LA$_{56}$-*b*-PEO$_{113}$ micelles loaded with lipophilic anticancer agent oxaliplatin were successfully produced with an encapsulation efficiency of 25.2%.

This work was supported by the Russian Science Foundation (project no. 21-73-00071). The authors are grateful to the resource centers of the National Research Center ‘Kurchatov Institute’ for the DSC, TGA, DLS, WAXS and SAXS experiments. The authors are grateful to PhD A. I. Kulebyakina and D. R. Streltsov from

the NRC ‘Kurchatov Institute’ for fruitful discussions, PhD A. A. Nazarov from M. V. Lomonosov Moscow State University for the synthesis of oxaliplatin and PhD V. K. Karandashev from the Institute of Microelectronics Technology and High-Purity Materials of the Russian Academy of Sciences (IMT RAS) for experiments with ICP-MS.

Online Supplementary Materials

Supplementary data associated with this article can be found in the online version at doi: 10.1016/j.mencom.2023.01.027.

References

1 R. Simonutti, D. Bertani, R. Marotta, S. Ferrario, D. Manzone, M. Mauri, M. Gregori, A. Orlando and M. Masserini, *Polymer*, 2021, **218**, 123511.
2 E. V. Razuvaeva, A. I. Kulebyakina, D. R. Streltsov, A. V. Bakirov, R. A. Kamyshinsky, N. M. Kuznetsov, S. N. Chvalun and E. V. Shtykova, *Langmuir*, 2018, **34**, 15470.
3 D. S. Dolgov, T. E. Grigor’ev, A. I. Kulebyakina, E. V. Razuvaeva, R. A. Gumerov, S. N. Chvalun and I. I. Potemkin, *Polym. Sci., Ser. A*, 2018, **60**, 902 (*Vysokomol. Soedin., Ser. A*, 2018, **60**, 522).
4 T. Riley, S. Stolnik, C. R. Heald, C. D. Xiong, M. C. Garnett, L. Illum, S. S. Davis, S. C. Purkiss, R. J. Barlow and P. R. Gellert, *Langmuir*, 2001, **17**, 3168.
5 Y. A. Kadina, E. V. Razuvaeva, D. R. Streltsov, N. G. Sedush, E. V. Shtykova, A. I. Kulebyakina, A. A. Puchkov, D. S. Volkov, A. A. Nazarov and S. N. Chvalun, *Molecules*, 2021, **26**, 602.
6 S. M. E. Kamrani and F. Hadizadeh, *J. Biomol. Struct. Dyn.*, 2019, **37**, 4215.
7 N. G. Sedush, Y. A. Kadina, E. V. Razuvaeva, A. A. Puchkov, E. M. Shirokova, V. I. Gomzyak, K. T. Kalinin, A. I. Kulebyakina and S. N. Chvalun, *Nanobiotechnol. Rep.*, 2021, **16**, 421.
8 E. V. Razuvaeva, K. T. Kalinin, N. G. Sedush, A. A. Nazarov, D. S. Volkov and S. N. Chvalun, *Mendeleev Commun.*, 2021, **31**, 512.
9 Yu. V. Ermolenko, A. S. Semyonkin, Yu. V. Ulianova, T. S. Kovshova, O. O. Maksimenko and S. E. Gelperina, *Russ. Chem. Bull.*, 2020, **69**, 1416.
10 K. Jelonek, J. Kasperczyk, S. Li, T. H. N. Nguyen, A. Orchel, E. Chodurek, P. Paduszyński, M. Jaworska-Kik, E. Chrobak, E. Bębenek, S. Boryczka, M. Jarosz-Biej, R. Smolarczyk and A. Foryś, *Int. J. Pharm.*, 2019, **557**, 43.
11 H. Soleymani Abyaneh, M. R. Vakili, A. Shafaati and A. Lavasanifar, *Mol. Pharmaceutics*, 2017, **14**, 2487.
12 K. Jelonek, S. Li, X. Wu, J. Kasperczyk and A. Marcinkowski, *Int. J. Pharm.*, 2015, **485**, 357.
13 C. Ma, P. Pan, G. Shan, Y. Bao, M. Fujita and M. Maeda, *Langmuir*, 2015, **31**, 1527.
14 L. Yang, X. Qi, P. Liu, A. El Ghzaoui and S. Li, *Int. J. Pharm.*, 2010, **394**, 43.
15 H. Niu, J. Li, Q. Cai, X. Wang, F. Luo, J. Gong, Z. Qiang and J. Ren, *Langmuir*, 2020, **36**, 13881.
16 L. Piao, Y. Li, H. Zhang and J. Jiang, *J. Biomater. Sci., Polym. Ed.*, 2019, **30**, 233.
17 N. Kang, M.-È. Perron, R. E. Prud’homme, Y. Zhang, G. Gaucher and J.-C. Leroux, *Nano Lett.*, 2005, **5**, 315.
18 L. Chen, Z. Xie, J. Hu, X. Chen and X. Jing, *J. Nanopart. Res.*, 2007, **9**, 777.
19 S. Li and M. Vert, *Macromolecules*, 2003, **36**, 8008.
20 I. G. Shin, S. Y. Kim, Y. M. Lee, C. S. Cho and Y. K. Sung, *J. Controlled Release*, 1998, **51**, 1.
21 E. Tomaszewska, K. Soliwoda, K. Kadziola, B. Tkacz-Szczesna, G. Celichowski, M. Cichomski, W. Szmaja and J. Grobelny, *J. Nanomater.*, 2013, 313081.
22 C. Garofalo, G. Capuano, R. Sottile, R. Tallerico, R. Adami, E. Reverchon, E. Carbone, L. Izzo and D. Pappalardo, *Biomacromolecules*, 2014, **15**, 403.
23 I. Akiba, N. Terada, S. Hashida, K. Sakurai, T. Sato, K. Shiraishi, M. Yokoyama, H. Masunaga, H. Ogawa, K. Ito and N. Yagi, *Langmuir*, 2010, **26**, 7544.
24 S. Noack, D. Schanzenbach, J. Koetz and H. Schlaad, *Macromol. Rapid Commun.*, 2019, **40**, 1800639.
25 D. Brizzolara, H.-J. Cantow, K. Diederichs, E. Keller and A. J. Domb, *Macromolecules*, 1996, **29**, 191.
26 J. Zhang, Y. Duan, H. Sato, H. Tsuji, I. Noda, S. Yan and Y. Ozaki, *Macromolecules*, 2005, **38**, 8012.

Received: 31st March 2022; Com. 22/6851